Experimental Thermal and Fluid Science 98 (2018) 362–368

Contents lists available at ScienceDirect

Experimental Thermal and Fluid Science

journal homepage: www.elsevier.com/locate/etfs

Study on coalescence dynamics of unequal-sized microbubbles captive on solid substrate

Shuyi Zhou[a], Yuanzhi Cao[a], Rou Chen[a], Tao Sun[b], Kamel Fezzaa[b], Huidan Yu[a], Likun Zhu[a,*]

[a] Department of Mechanical Engineering, Indiana University–Purdue University Indianapolis, Indianapolis, IN 46202, USA
[b] Advanced Photon Source, Argonne National Laboratory, Argonne, IL 60439, USA

ARTICLE INFO

Keywords:
Bubble coalescence
Synchrotron
High-speed X-ray imaging
Bridging neck growth
Surface wave propagation
Microfluidic

ABSTRACT

The dynamics of bubble coalescence are of importance for a number of industrial processes, in which the size inequality of the parent bubbles plays a significant role in mass transport, topological change and overall motion. In this study, coalescence of unequal-sized microbubbles captive on a solid substrate was observed from cross-section view using synchrotron high-speed imaging technique and a microfluidic gas generation device. The bridging neck growth and surface wave propagation at the early stage of coalescence were investigated by experimental and numerical methods. The results show that theoretical half-power-law of neck growth rate is still valid when viscous effect is neglected. However, the inertial-capillary time scale is associated with the initial radius of the smaller parent microbubble. The surface wave propagation rate on the larger parent microbubble is proportional to the inertial-capillary time scale.

1. Introduction

Coalescence of microbubbles are encountered in many industrial applications when gas microbubbles are generated from or injected into liquid reactants, such as solar water splitting systems [1–3], microbial electrolysis cells [4–6], and gas-liquid synthesis [7–9]. Fundamental understanding of coalescence dynamics of microbubbles is essential to the design of those systems and devices. To this end, most studies on microbubble coalescence have been focused on equal-sized parent bubbles with a complete spherical shape. For instance, the dynamics of thinning and rupture of the liquid film between two approaching bubbles just prior to coalescence have been studied extensively [10–14]. The dynamics of bridging neck growth have been the focus of many studies [15–19]. It has been shown that the bridging neck radius r of two parent bubbles follows a power-law, $r/R \propto (t/\tau)^{1/2}$, at the early-stage of coalescence, where R is the initial radius of parent bubbles and τ is a time scale. When viscous effect is negligible, the time scale is inertial-capillary time scale $\tau = (\rho R^3/\sigma)^{1/2}$, where ρ is the density of liquid and σ is the surface tension [17]. Stover et al. investigated the effects of bubble size, electrolyte viscosity, and surface tension on the oscillation dynamics of a coalesced bubble [20]. They found that fluid inertia sustains the oscillation of the resultant bubble and viscous resistance dampens the oscillation. The oscillation period increases and damping decreases with increasing bubble size. Within the viscosity range from 1.1×10^{-2} cm^2/s to 5.0×10^{-2} cm^2/s, the oscillation frequency is insensitive to the viscosity and damping is insensitive to surface tension. Coalescence does not depend on gas type or electrolyte pH. These studies using equal-sized spherical bubbles have provided useful information on the dynamics of microbubble coalescence. However, in real applications, coalescence could happen when microbubbles are captive on a solid substrate with a spherical segment shape. In addition, the parent bubble sizes are different for most of the coalescence cases. Recently, Weon et al. have reported that the location of the coalesced bubble is linked by the parent bubble size ratio with a power-law relationship [21,22]. Chen et al. reported that the coalescence time also exhibits a power-law scaling with the parent bubble size ratio [23]. Zhang et al. studied the generation of a satellite during the coalescence of two gas bubbles. They found that the relative size of the parent bubbles has a critical effect on the generation of satellite, preventing it if this ratio is too large or too small [24]. However, the dynamics in the early-stage of coalescence of two unequal-sized microbubbles captive on a solid substrate have not been studied. The objective of this paper is to investigate whether there exists a universal time scaling law in such coalescence cases. In this study, the coalescence of two unequal-sized microbubbles captive on a solid substrate was investigated experimentally and numerically. A polymer microfluidic device was designed and fabricated to generate microbubbles and bubble coalescence events. A high-speed X-ray imaging instrument

* Corresponding author at: Department of Mechanical Engineering, Indiana University Purdue University Indianapolis, 723 W. Michigan Street, Room SL 260 L, Indianapolis, IN 46202, USA.
E-mail address: likzhu@iupui.edu (L. Zhu).

https://doi.org/10.1016/j.expthermflusci.2018.06.016
Received 28 September 2017; Received in revised form 2 May 2018; Accepted 20 June 2018
Available online 21 June 2018
0894-1777/

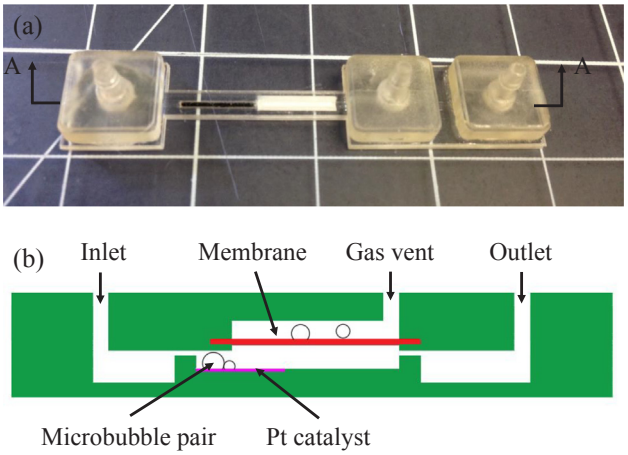

Fig. 1. (a) A picture of the fabricated polymer microfluidic gas generation device and (b) schematic of the cross-section view of the device.

at the 32-ID-B beamline of the Advanced Photon Source (APS) at Argonne National Laboratory was used to visualize individual coalescence events inside the polymer microfluidic channel. The bridging neck growth and surface wave propagation at the early stage of bubble coalescence were analyzed based on the X-ray images and simulation results.

2. Experimental

The coalescence experiment was carried out through microbubbles generated inside a polymer microfluidic gas generation device. The device was fabricated by aligning and sequentially stacking/thermo-press bonding multiple layers of patterned polystyrene (PS) film (Goodfellow, Coraopolis, PA) which were achieved by a craft cutter (FC2250-60 VC, Graphtec, Santa Ana, CA) [25]. A picture of the device and the schematic of a cross-section view of the device are shown in Fig. 1. A reaction microchannel was formed by bonding a platinum (Pt) black catalyst layer inside the microchannel. The Pt black was electroplated on a gold foil (10 μm thick) with 0.1 A/cm^2 current density for 55 s. The plating bath consisted of 120 ml of DI water and 5 g of dihydrogen hexachloroplatinate ($H_2PtCl_6{\cdot}6H_2O$, Alfa AESAR, Ward Hill, MA) [26]. The Pt density was measured and calculated to be 1.5 mg/cm^2. The gold foil was attached on a double-sided tape when being electroplated with Pt. Then it can be attached to PS film with the other adhesive surface, as is shown in Fig. 1(b). In order to vent the gas bubble in the reaction channel, a hydrophobic nanoporous membrane (0.2 μm pore size, Sterlitech Corporation, Kent, WA) was embedded into the device, as is shown in Fig. 1(b).

High-speed X-ray imaging experiments were conducted at the 32-ID-B beamline of APS to visualize individual coalescence events in the reaction channel. The experimental setup is illustrated in Fig. 2(a). An intense undulator white-beam went through the reaction channel of the device and generated phase-contrast images of the sample. A LuAG:Ce scintillator (100 μm thickness), positioned downstream, absorbed the X-ray photons and emitted visible light, which was then recorded by a high-speed camera (FastCam SA1.1, Photron) with 10^5 fps and 3 μs exposure time, as is shown in Fig. 2(b). It should be noted that the coalescence events were visualized from the cross-section view in this study. Since the parent microbubbles were captive on the Pt catalyst substrate with 36° contact angle, the top view cannot reveal the detailed dynamic information of bubble coalescence. In order to gain better image contrast, the longitudinal dimension of the reaction channel should be as small as possible to reduce the X-ray absorption by channel walls and liquid reactant, as is shown in Fig. 2(c). In this study, the rectangular reaction channel width was 0.7 mm with 1.15 mm PS wall on each side and the channel height was 144 μm. 30% hydrogen peroxide (H_2O_2) was used as reactant solution in this experiment. Oxygen generation reaction happened when the H_2O_2 solution was brought into contact with the Pt catalyst inside the reaction channel. To avoid the influence of X-ray on H_2O_2, we optimized the X-ray dose to make sure H_2O_2 didn't have obvious self-reaction under existence of the X-ray while the contrast of the image remained clear. As shown in Fig. 2(e), the phase-contrast X-ray image clearly shows the profiles of microbubbles and other substances with 2 μm spatial resolution.

The measurement of bridging neck growth and surface wave propagation based on X-ray images was aided by open software, ImageJ (National Institutes of Health). The detailed information about image processing and measurement uncertainty is shown in Fig. 3. As shown in Fig. 3a, the bubble center locations were determined before the bubbles started coalescence. Since the bubbles were at equilibrium before coalescence, their 3D shape should be perfect spherical segment and their 2D projection images shown in Fig. 3a should be perfect circular segment. To determine the location of the center, we have to find the boundary of the circular segment. As shown in Fig. 3b and c, a median filter in ImageJ (Despeckle) was used to remove the salt and pepper noise by replacing each pixel with the median value in its 3 × 3 neighborhood. Fig. 3d shows the gray value profile along the solid line shown in Fig. 3c. We selected the pixel with the lowest gray value to be the boundary. After the boundary of the circular segment was determined, the center can be determined. Since the pixel size is 2 μm in this study, the uncertainty of the center location is 2 μm.

3. Results and discussion

The high-speed synchrotron X-ray imaging technique allowed the direct observation of the captive microbubble coalescence inside the reaction channel from the cross-section view, due to the small wavelengths of hard X-rays (~0.1 nm) [27]. In addition, this microfluidic gas generator enables the cross-section view of captive bubbles on the solid substrate. Fig. 4 shows an example of the coalescence of two unequal-sized microbubbles. The whole coalescence process took place in 170 μs. A series of images have been taken by the high-speed camera at a frame rate of 10^5 fps. Since H_2O_2 solution had flow motions inside the reaction channel and oxygen generation took place continuously during the imaging process, it is necessary to identify whether the flow motion and oxygen generation had impact on the individual coalescence event. It can be seen from the images in Fig. 4 that all other bubbles do not have clear change during the 170 μs time span. Therefore, we can conclude that the flow motion and oxygen generation were at a relatively low speed and they don't have impact on individual coalescence event. In Fig. 4 at 0 μs, two microbubbles, with radius 64 μm and 36 μm respectively, were about to contact each other. The coalescence of the two microbubbles took place in a very short period of time and in the next frame at 10 μs, the two microbubbles have formed a bridging neck, with an arch shape in the middle. It should be noted that the coalescence events were selected from the video of gas generation in the microchannel. In this experiment, the start of a coalescence event cannot be controlled. Since the temporal resolution of the high-speed camera was 10 μs, the uncertainty in determining the initial time (0 μs) was 10 μs. 10 μs uncertainty is relative large for this study. In order to address this issue, the experimental results and simulation results were compared when selecting the coalescence events and determining the initial time. As show in Fig. 5, the simulation results show similar time as the experimental when they have the similar neck growth. From 10 μs to 60 μs, it is observed that a surface wave on the liquid-gas interface travels on the larger bubble. During this period, the